Journal of Materials Science: Materials in Electronics (2019) 30:2351–2359
https://doi.org/10.1007/s10854-018-0508-9

Optimized nc-Si:H thin films with enhanced optoelectronic properties prepared by micro-waves PECVD used as an effective silicon surface passivation layer

Seif El Whibi[1,2,3] · Lotfi Derbali[1] · Pascal Tristant[3] · Cedric Jaoul[3] · Maggy Colas[3] · Richard Mayet[3] · Julie Cornette[3] · Hatem Ezzaouia[1]

Received: 14 August 2018 / Accepted: 4 December 2018 / Published online: 11 December 2018
© Springer Science+Business Media, LLC, part of Springer Nature 2018

Abstract

In this work we investigated a novel approach to elaborate hydrogenated nanocrystalline silicon (nc-Si:H) thin films using microwave plasma enhanced chemical vapor deposition (MW-PECVD) system, used as an efficient silicon surface passivation layer. We studied the effect of the hydrogen flow rate on the structural, morphological and optical properties of nc-Si:H thin films. Obtained results confirm its crucial role on the properties of the resulted thin films. Optimized hydrogen flow rate allowed an hydrogenated nanocrystallites (nc-Si:H) with around 80% of a crystallization phase which is a high percentage compared to previous works. The XRD analysis was supported by Raman spectroscopy, indicating the pure phase of cubic structure with a preferred orientation along (111) plane. The average grain size was found to vary between 7 and 16 nm. The surface morphology of the deposited thin films was carried out using atomic force microscopy (AFM), showing a clear dependence of surface roughness with the hydrogen flow rate. The refractive index of the obtained thin films was evaluated by means of the Bruggeman effective medium approximation (BEMA). The optical band gap and the porosity of the films were deduced from spectroscopic ellipsometry measurements and results were found strongly correlated with XRD and AFM analysis respectively. Moreover, the minority carrier lifetime measurements (MCL) prove the effectiveness of the subjected treatment for a high quality nc-Si:H thin film and its crucial role as a passivation layer of crystalline silicon substrate, revealing a significant improvement of their optoelectronic properties.

1 Introduction

The hydrogenated nanocrystalline silicon (nc-Si:H) is a mixed phase material consisting on the deposition of embedded silicon nanocrystallites into an amorphous matrix. The nc-Si:H thin films are a promising candidate for the fabrication of high performing optoelectronic devices such as thin films solar cells [1, 2, thin films transistors (TFT) [2] and novel electronic devices [3]. Compared to hydrogenated amorphous silicon (a-Si:H), this material (nc-Si:H) has become a very suitable semiconductor for increasing the carrier mobility allowing the improvement of TFT stability and higher efficiency of solar cells conversion through the reduction of carrier recombination [4, 5]. Besides, hydrogenated nanocrystalline silicon thin films present very interesting optical properties for photovoltaic devices compared to a:Si-H: larger band gap energy and a near direct band gap [6]. In addition to those qualities, nc-Si:H thin films contribute to a stable passivation of silicon by neutralizing of danging bonds and the removal of trapping states [7]. Those properties depend essentially on the nanocrystallite size and the fraction of the crystalline phase of the films. Consequently, the deposition parameters of nc:Si-H thin films plays a crucial role for obtaining the desirable physical properties allowing higher solar radiation absorption without affecting the series resistance [8]. Several techniques were used to elaborate hydrogenated nanocrystalline silicon thin

✉ Lotfi Derbali
l.derb@yahoo.fr

[1] Laboratory of Semiconductors, Nanostructures and Advanced Technologies (LSNTA), Research and Technology Center of Energy (CRTEn), Technopol of Borj-Cedria, BP 95, 2050 Hammam-Lif, Tunisia

[2] Faculty of sciences of Bizerte, University of Carthage, 7021 Zarzouna, Tunisia

[3] Institute of Research on Ceramics, IRCER - UMR 7315, Université de Limoges, Centre Européen de la Céramique, 12 rue Atlantis, 87068 Limoges Cedex, France

films such as very high frequency (VHF) PECVD [9], hot wire chemical vapor deposition (HW-CVD) [10], electron cyclotron resonance (ECR) CVD [11], and low-pressure chemical vapor deposition (LPCVD) [12]. In this work, micro-waves plasma enhanced vapor deposition (MW-PECVD), which is a promising deposition technique for a various type of materials, was used to elaborate nc:Si-H thin films. The influence of optimized hydrogen flow rate on the structural, optical and morphological properties was investigated. Also, with MCL measurements, we will prove the efficiency of this novel elaboration method as an efficient passivation route of crystalline silicon substrate for an enhanced optoelectronic properties.

2 Experimental details

Hydrogenated nanocrystalline silicon nc-Si:H thin films were deposited using micro-waves PECVD on p-type monocrystalline (100) silicon substrate (Cz, 5–10 Ω cm). A mixture of SiH_4, H_2 and Ar was used as precursor gases. The silicon precursor gas is diluted in Ar environment with $[SiH_4]/[Ar] = 5\%$. The silicon wafers were cleaned in a CP4 solution which contains: 64% HNO_3, 16% HF and 20% CH_3COOH during 20 s then, they was rinsed with deonized water. The second step of cleaning the silicon substrates (c-Si) consisted on rinsing them with acetone and ethanol respectively, then in deonized water. The nc-Si:H thin films were deposited with a fixed flow rates of Ar and SiH4 equal to 151 and 60 sccm respectively, and the substrate temperature was kept fixed with the micro-waves power at 250 °C and 1000 W respectively. In order to study the effect of hydrogen gas on the properties of the films, different flow rates of hydrogen was introduced during the synthesis of nc-Si:H thin films. XRD measurements were obtained using Bruker D8 advance (Cu Kα line λ = 1.54056 Å). The crystalline volume fraction and films vibrational modes of the samples were studied using Raman spectroscopy (Jobin–Yvon spectrometer T 64,000 model equipped with a CCD camera cooled, 488 nm wavelength laser). The FTIR spectra of nc-Si:H thin films were recorded using FTIR spectrophotometer (OMNIC) to investigate the configuration of silicon hydrogen bonding in the infrared region 500–2500 cm^{-1}. The surface morphology of nc-Si:H was studied using an atomic force microscopy (AFM) using the tapping AFM mode. The spectroscopic ellipsometry (SE) measurements were made using an ex situ spectroscopic ellipsometer (Sopra model) equipped with goniometer in the range of 250–840 cm^{-1} at incidence angle of 70°. Finally, minority carrier lifetime (MCL) measurements were carried out with a WCT-120 photo-conductance lifetime tester [13].

3 Results and discussion

3.1 Structural properties

The X-ray diffraction (XRD) patterns of the prepared nc-Si:H thin films with different hydrogen flow rates (FH_2) are reported in Fig. 1. The obtained results indicates the presence of three well defined peaks located at 28.4°, 47.3° and 56° assigned to (111), (220) and (311) lattice planes respectively of the cubic Si structure. The films have a preferential growth along (111) plane and the intensity of this diffraction peak increases as we increase the hydrogen flow rate. This behavior is highlightened through the RAMAN spectroscopy measurements illustrated in Fig. 3 [14]. The texture coefficient ($TC_{(hkl)}$) was introduced in order to indicate the preferred orientation of the prepared samples, shown in Fig. 2. This parameter gives an idea about the number of grains along the considered (hkl) plane and a rise of $TC_{(hkl)}$ is a result of an increased number of grains along the studied (hkl) plane. The texture coefficient of the prepared thin films were estimated using the following equation:

$$TC_{(hkl)} = \frac{I_{(hkl)}/I_{0(hkl)}}{N^{-1}\sum_N I_{(hkl)}/I_{0(hkl)}} \quad (1)$$

where $I_{(hkl)}$is the intensity of the (*hkl*) plane of the thin film, $I_{0(hkl)}$ is the intensity of (*hkl*) plane of the reference sample taken from the JCPDS 27-1402 card, and *N* is the number of diffraction peaks under consideration. Samples that present $TC_{(hkl)} > 1$ exhibit a preferred orientation along that plane, and samples with randomly oriented grains imply$TC_{(hkl)} \approx 1$. The preferred growth of the Si-H films changes from (311) plane to (111) plane with increasing FH_2 with$TC_{(311)} > 1$ for 19 and 29 sccm and $TC_{(220)} > 1$ for 39 sccm. On the basis of

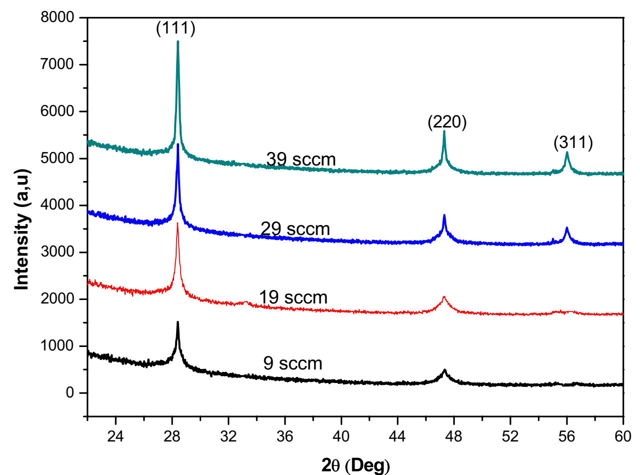

Fig. 1 The X-ray spectra of nc-Si:H films deposited under different hydrogen flow rates

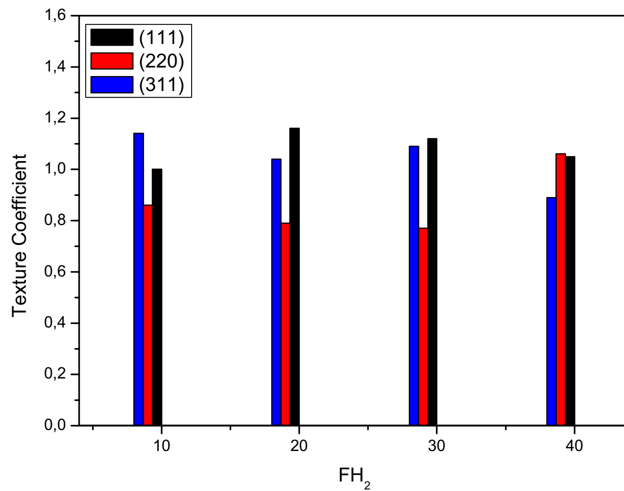

Fig. 2 Texture Coefficient ($TC_{(hkl)}$)

The obtained Raman spectra were recorded in the range of 450–550 cm^{-1} as illustrated in Fig. 3, showing the presence of an asymmetric broad peak describing a mixture of two phases: amorphous and nanocrystalline structures [15], for all the prepared nc-Si:H thin films.

In order to obtain more details about the structural phases of the films, the obtained Raman spectra of the prepared samples were deconvoluted and fitted as a sum of three Gaussian component peaks as indicated in Fig. 4. The first peak located at around 480 cm^{-1} correspond to TO vibrational mode of a-Si:H (amorphous hydrogenated silicon phase) and the second peak (500–510 cm^{-1}) corresponds to an intermediate structural phase with the presence of the thermodynamically stable ultra-nanocrystalline grains (1 to 2 nm) [16]. It was also reported by other authors that this peak can also be assigned to the dilatation of the Si–Si bonds near the grain boundaries [17]. The third Gaussian

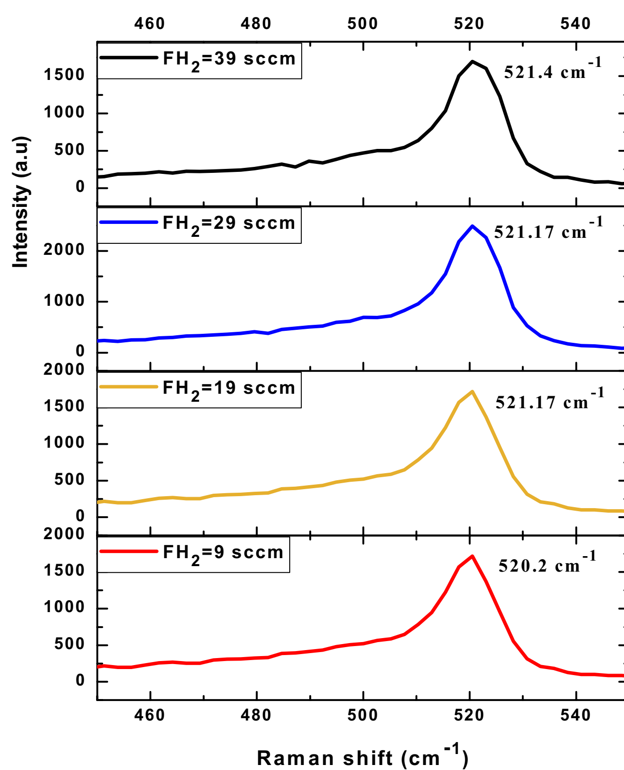

Fig. 3 Raman spectra of the nc-Si:H films at various hydrogen flow rates

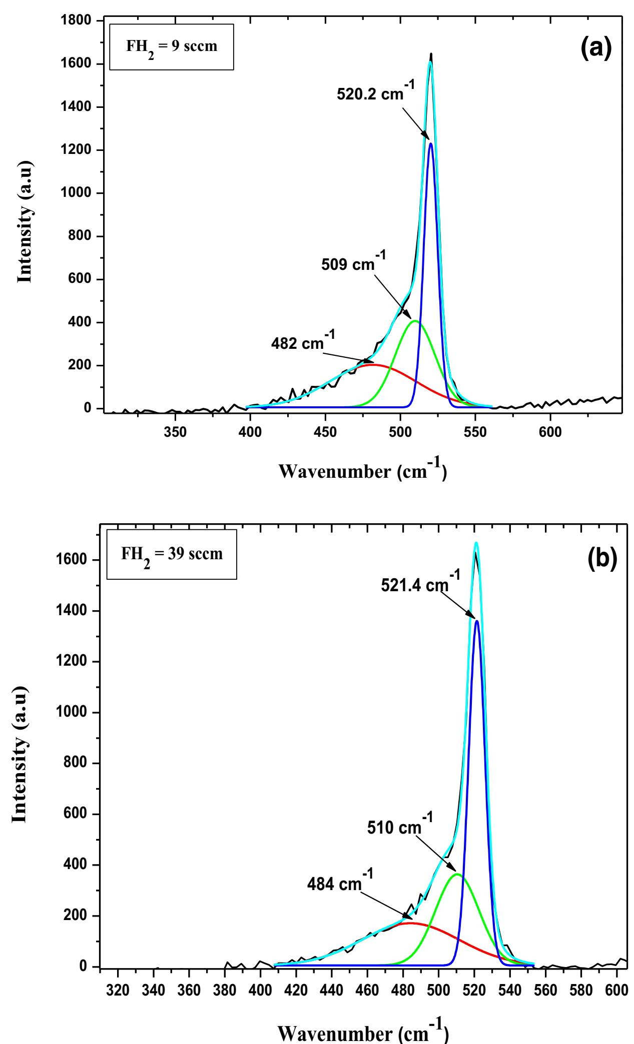

Fig. 4 Typical deconvoluted Raman spectrum of deposited films at hydrogen flow rates **a** FH = 9 sccm and **b** FH = 39 sccm

the obtained results, a small change in the hydrogen flow rate contributes to significant modification of the grain growth in the deposited films.

Raman spectroscopy is a sensitive and powerful technique allowing the identification of structural properties of amorphous-crystalline mixed phase silicon based thin films.

peak located around 520–521 cm^{-1} is attributed to the pure nanocrystalline phase of Si-H TO vibrational mode which is the matter of interest of this work. In order to estimate the percentage of this crystalline phase, the nanocrystallite volume fraction (Fc) was evaluated using the following formula [18].

$$F_c = (I_2 + I_3)/(I_1 + I_2 + I_3)$$

where I_1, I_2 and I_3 are the integrations of the peaks associated to the crystalline phase, the intermediate phase, and the amorphous phase respectively. Furthermore, we estimated the crystallite size of nc-Si:H thin films using this equation [19]:

$$d_{Ram} = 2\pi\sqrt{\frac{B}{\Delta\omega}}$$

where $\Delta\omega$ is the peak shift compared to the c-Si and B is a constant equal to 2.24 cm^{-1} nm^2 for silicon [20].

As seen in Table 1, the effect of increasing the flow rate of hydrogen during the synthesis of nc-Si:H is clearly seen through the shift of the third Gaussian peak's position from 520.2 to 521.4 cm^{-1}. The variation of FH_2 can be accompanied by an expansion of crystallite size values as listed in Table 1. Both latter phenomena lead us to deduce that a higher hydrogen flow rate promotes the formation of Si–Si bonds.

3.2 FTIR spectroscopic analysis

To investigate the influence of H_2 flow rates on the chemical structure of nc-Si:H thin films, FTIR measurements were carried out in transmission mode and the obtained curves are shown in Fig. 5. In this figure, we can notice the presence of well-defined absorption peaks corresponding to various vibrational modes of Silicon-Hydrogen bands. Bands appearing at 621 cm^{-1} and 854 cm^{-1} are attributed to the Si-H_n wagging mode [21, 22] and to the Si-H_2/ (Si-$H_2)_n$ bending vibration mode (isolated or coupled) [20, 22], respectively, as indicated in Fig. 5. A band corresponding to the stretching vibrational mode of Si–O–Si was obtained

Table 1 Peak's position of the third Gaussian component, crystalline volume fraction and crystallite size of nc-Si:H thin films at different hydrogen flow rates extracted from the RAMAN spectroscopy measurements

Hydrogen flow rates (sccm)	Peak's position (cm^{-1})	Crystalline Volume Fraction: F_c (%)	Crystallites size d_{Ram} (nm)
9	520.2	89.17	7.57
19	521.07	88.31	11.48
29	521.17	90	12.44
39	521.4	91.16	16.11

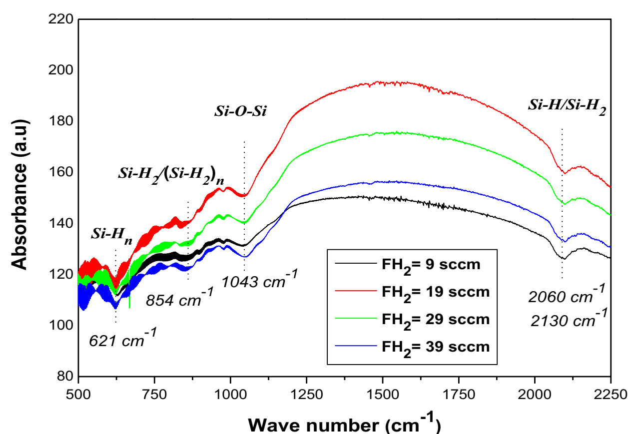

Fig. 5 FTIR transmission spectra of nc-Si:H films deposited at different hydrogen flow rates

in all the FTIR spectra [23]. Furthermore, we can notice the presence of a broad absorption band located at about 2100 cm^{-1} for all the made thin films, which corresponds to the superposition of two absorption bands : stretching vibrational modes of both Si–H at 2060 cm^{-1} and Si–H_2/(Si–$H_2)_n$ complexes at 2130 cm^{-1} [24, 25]. The intensity of absorption bands exhibit a decreasing tendency with increasing the hydrogen flow rate, showing that higher introduced FH_2 during the synthesis of the films reduce the amount of Si-H bonds. This correlates well with the previously reported results in the structural analysis. Indeed, more the amount of Si–H bonds is reduced, more the Si–Si bonds are likely to be formed. This behavior can be explained by the chemical annealing model that consist of chemical reactions between the hydrogen spices present in the plasma and the silicon-bonded hydrogen at the surface and inside the deposited thin films [25]. Thus, this process includes the formation of H_2 molecules through the recombination of the hydrogen species in the plasma and the hydrogen species present in the film.

3.3 AFM surface analysis

We investigated the surface morphology of the deposited thin films by means of the Atomic Force Microscopy (AFM) and the obtained images 2D are illustrated in Fig. 6a, b. All the deposited nc-Si:H thin films by micro-waves PECVD exhibit small spherical shape clusters. It is clearly seen in Fig. 6a that the smallest hydrogen flow rate contributed to homogeneous and uniform hydrogenated silicon nanocrystals compared to those with higher flow rates that tends to form agglomerated clusters as specially seen in Fig. 6d. This can be caused by the reduction of Si–H bonds with higher FH_2 that promotes the nucleation of silicon nanocrystals. The root-mean-square (RMS) roughness of the prepared thin

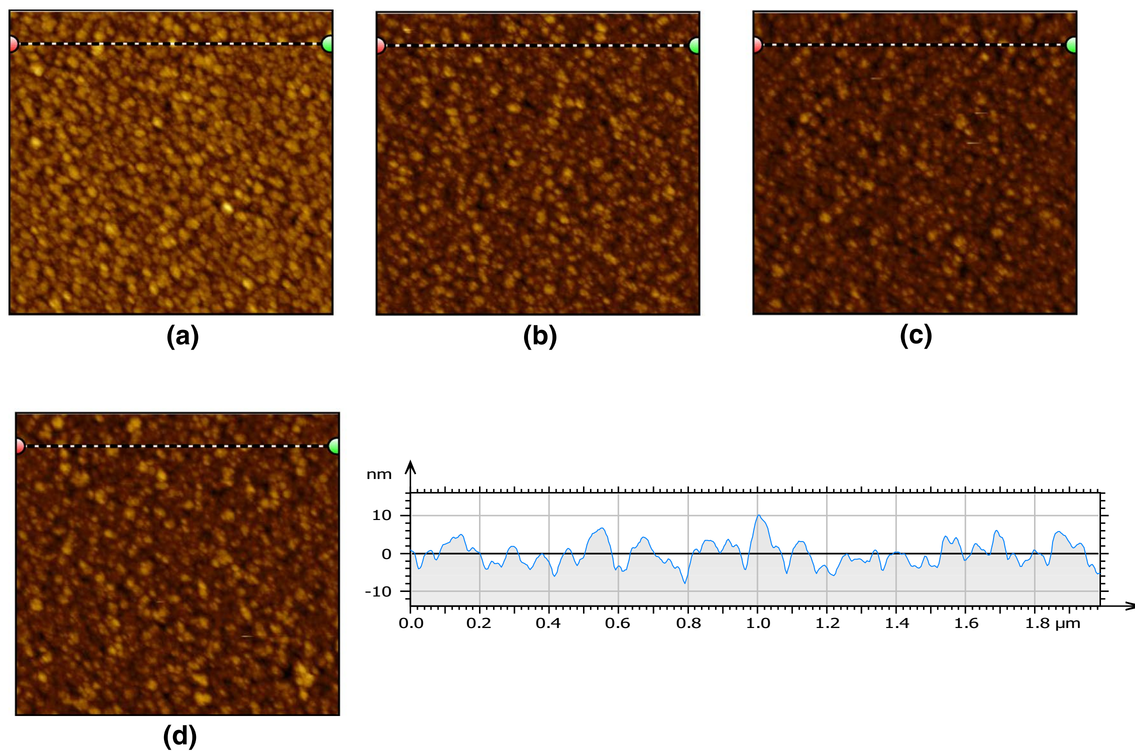

Fig. 6 Surface morphology of nc-Si:H films deposited at different value of hydrogen flow rates: **a** FH = 9 sccm, **b** FH = 19 sccm, **c** FH = 29 sccm, **d** FH = 39 sccm

Table 2 The Root-mean-square (Rms) roughness and the average grain size from AFM study as a function of hydrogen flow rates

H_2 flow rates (sccm)	Root mean square Rms (nm)	Average grain size (nm)
9	2.60	9.81
19	2.69	12.73
29	2.84	14.9
39	3.34	17.46

films was evaluated and the results are listed in Table 2. We estimated the crystallite size from the AFM data, and found to be close to the calculated values presented in Table 1 deduced from Raman analysis. The surface roughness of the films also increased with the crystallite size, deduced from Raman analysis, confirming the formation of nucleated silicon clusters on the surface. The latter has a significant impact on the optical properties of the deposited nc-Si:H thin films that presents an important matter of interest for the performance of these samples in many application fields.

3.4 Spectroscopic ellipsometry

Spectroscopic ellipsometry measurements were performed to investigate the evolution of nc-Si:H optical properties with the variation of the hydrogen flow rate (FH_2). The obtained variations of the two spectroscopic angles Ψ and Δ, as shown in Fig. 7a, b, are attributed to some apparent variations on the films properties after increasing FH_2: thickness and surface roughness [26]. The obtained results were fitted using the effective medium approximation models (EMA), and among those models, the Bruggeman function was found to be the appropriate one to extract and study the optical properties of the prepared thin films as shown in Fig. 8. The Bruggeman model assumes that all constituents of the material are considered as randomly arranged spherical inclusions, and since the deposited samples has intermediate structural phases, the percentage of each phase was taken into consideration from the Raman spectroscopic analysis. Furthermore, the fitting was performed considering multilayer thin films as illustrated in Fig. 9 [27]. The mean-square deviation and the regression coefficient were found to be $\sigma < 0.001$ and $R^2 > 0.99$ respectively showing higher agreement between the fitted and the measured results. Table 3 show the variation of some parameters deduced from Bruggeman analysis.

The reflective index (n) and the extinction coefficient (k) were deduced from spectroscopic ellipsometry measurements and are reported in Fig. 10a, b. It is shown that increasing FH_2 values increased the refractive index and extinction coefficient of the films. This can be due to the

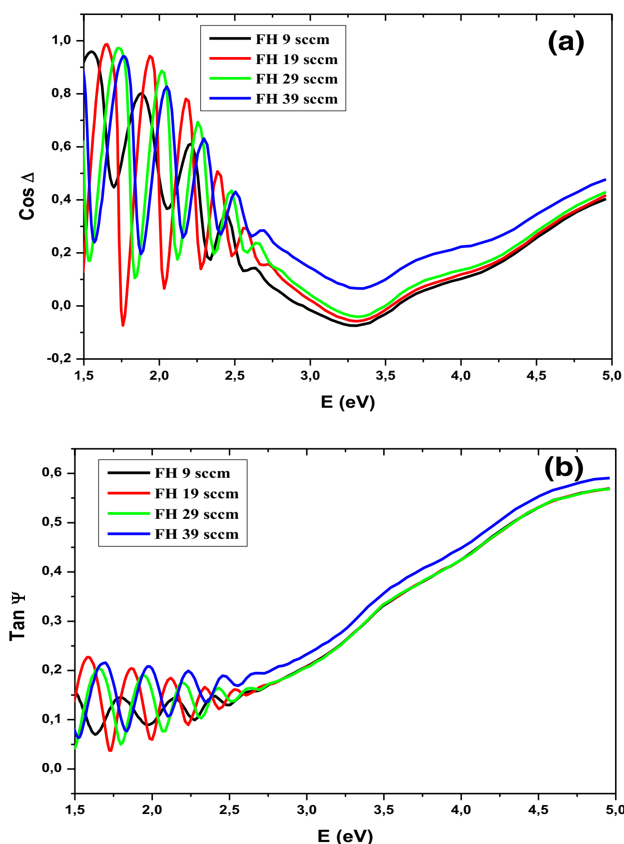

Fig. 7 Measured spectroscopic ellipsometry: Cos Δ (**a**) and Tan Ψ (**b**) of the deposited nc-Si:H thin films at different values of hydrogen flow rate (FH_2)

higher density of nucleated silicon atoms on the surface due to the small reduction of Si-H bonds. The increase of the optical constants can be related to the decrease of film's thickness with higher FH_2 as seen in Table 4. The optical band gap energy of the films was estimated using the Tauc's plot method and the obtained values are listed in Table 4 [28]. Varying the introduced hydrogen flow rate during the elaboration of nc-Si:H thin films decreased the band gap values from 1.54 eV to 1.36 eV. Those results are consistent with the calculated crystallite size in the structural analysis. Indeed, one of the characteristics of the quantum confinement effect is that a small change in the grain size distribution can higher affect the optical properties of materials.

It was reported in the experimental procedure that the deposition time of nc-Si:H is the same for all samples prepared with different FH_2. The obtained film thickness decrease is suggested to be attributed to the chemical annealing model process that contributes to the formation of H_2 molecules through hydrogen plasma species and the hydrogen atoms on the films, as mentioned in FTIR analysis.

Figure 11 shows the evolution of the imaginary dielectric constant (ε_2) at different hydrogen flow rates for the prepared nc-Si:H thin films. It was reported that in the low energy region (< 2.1 eV), the variation of ε_2 is related to both of the substrate properties and the thickness of the films, while at high energies (> 2.1 eV), ε_2 changes are assigned to the bulk composition and surface roughness [29]. Based on the literature, the imaginary part of the dielectric constant (ε_2) spectra presents generally two strong shoulders at around 3.4 and 4.2 eV corresponding to the critical points (CP) of the crystalline silicon structure [29]. In Fig. 11 we can notice the presence of two strong peaks located at 2.19 and 3 eV clearly seen for higher FH_2 rates. The increased intensity of the appearing peaks with FH_2 in Fig. 10 is highly consistent with the structural study, since the nanocrystalline phase raised obviously with increasing the hydrogen flow rates (FH_2).

3.5 Minority carrier lifetime

Lifetime carrier measurements of the films were estimated using the WCT-120 photo-conductance lifetime tester developed by Sinton and Cuevas [30] in order to study the passivation role of nc-Si:H/c-Si and the effect of the deposition parameters on the silicon substrate optoelectronic properties. The effective carrier lifetime τ_{eff} was measured by means of transient mode of the photoconductance decay (PCD) method. The minority carrier lifetime is considered as an important parameter that defines the quality of the crystalline silicon substrates. The measured τ_{eff} takes into account the recombination mechanisms that occurs at both surfaces of the sample as well as within its bulk. The defects at the surface of substrates are mainly produced by the interruption to the periodicity of the crystal lattice, which engenders dangling bonds at the semiconductor surface. The reduction of the number of dangling bonds, and hence the recombination, at the surfaces of the substrates, was achieved by growing the optimized nc-Si:H thin film onto the front surface of the silicon substrates. The reduction of dangling bonds is known as surface passivation, which leads to an important decrease of the surface recombination. The measurements were made at room temperature with an injection of a carrier density equal to $\Delta n = 10^{14}$ cm^{-3}. The extracted values of the effective lifetime (τ_{eff}) can be described as a measure of the surface passivation quality of the silicon substrate surface after the deposition of the hydrogenated nanocrystalline silicon films (nc-Si:H). Considering a uniform carrier generation in the silicon wafer, the effective lifetime carriers of the films can be expressed as follow [31]:

$$\frac{1}{\tau_{eff}} \approx \frac{1}{\tau_{bulk}} + \frac{2S_{eff}}{W}$$

τ_{bulk} is the bulk minority carrier lifetime. τ_{eff} is the resulting total effective minority carrier lifetime.

Fig. 8 Ellipsometric spectra and corresponding theoretical fit for a deposition flow rate 9 sccm

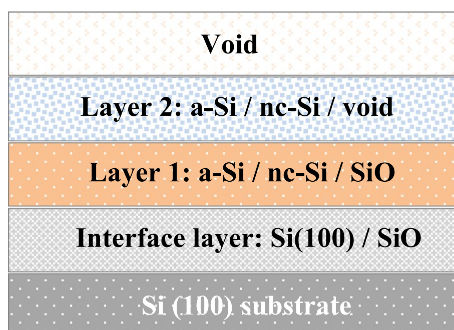

Fig. 9 Schematic illustration of the optical multilayer modeling steps from spectroscopic ellipsometry measurements

Figure 12 shows the evolution of the minority carrier lifetime (MCL) with different FH_2 rates. A significant enhancement of the MCL values was obtained for all the prepared samples compared to the untreated silicon substrate (reference). The latter was found to be obviously higher than those obtained in previous works [32–34]. The improved MCL values indicate the important and valuable role of introducing hydrogen atoms during the deposition of silicon nanocrystals onto the surface of the silicon substrate, which allowed an efficient passivation process of the dangling bonds and promoted the reduction of surface state density leading to an obvious decrease of the recombination activities.

Table 3 Parameters values obtained from the Brugemman EMA analysis

FH_2 (sccm)	Energy band gap (eV)	Cristallite size (nm)	Thickness layer (nm)	Nanocristalline volume fraction (%)	Amorphous volume fraction (%)	Void volume fraction (%)	Deposition rates (nm min^{-1})
9	1.54	7.57	366	89.17	6.53	4.3	18.3
19	1.50	11.48	355	88.31	6.49	5.2	17.75
29	1.39	12.44	332	90	3.7	6.3	16.6
39	1.36	16.11	328	91.16	1.63	7.21	16.4

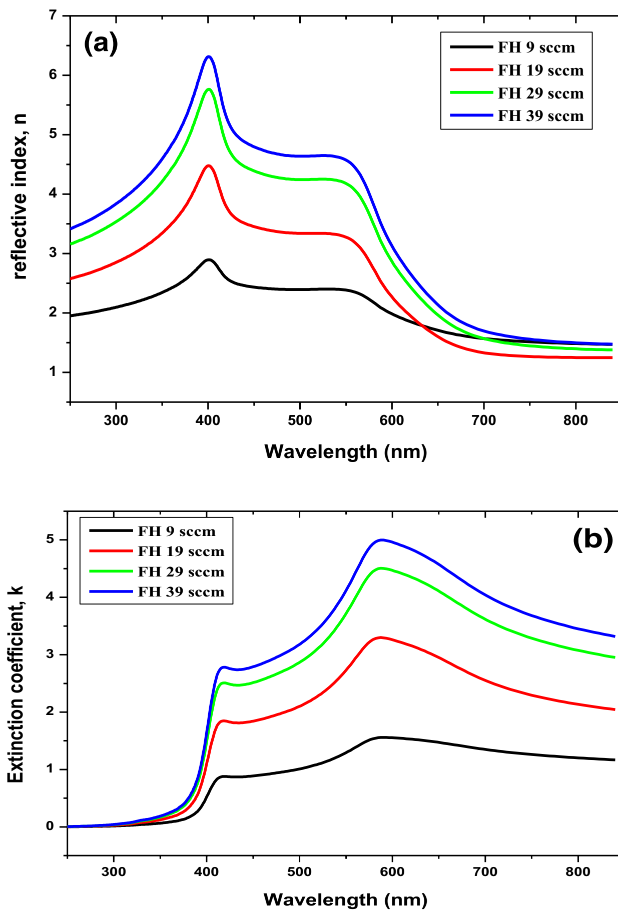

Fig. 10 Evolution of refractive index (**a**) and extinction coefficient (**b**) of the deposited nc-Si:H thin films with different hydrogen flow rate

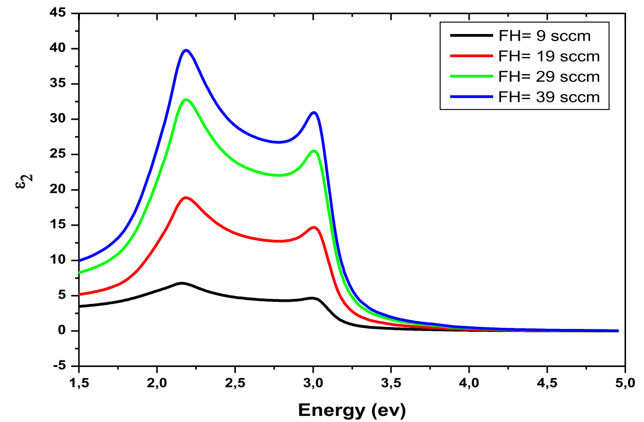

Fig. 11 Variation of the imaginary dielectric constant of nc-Si:H thin films with hydrogen flow rate (FH_2)

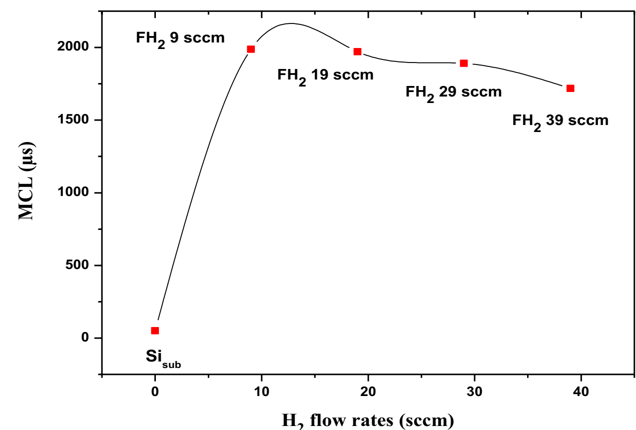

Fig. 12 Evolution of minority carrier lifetime in the deposited nc-Si:H thin films for different hydrogen flow rates

Table 4 Evolution of energy band gap, thickness and deposition rates of the deposited nc:Si-H with FH_2

FH_2 (sccm)	Energy band gap (eV)	Thickness (nm)	Deposition rates (nm min^{-1})
9	1.54	366	18.3
19	1.50	355	17.75
29	1.39	332	16.6
39	1.36	328	16.4

The resulting improvement of MCL indicates the crucial role of Hydrogen atoms in the nc-Si:H film to reduce the surface defect state density and dangling bonds and therefore leads to the reduction of carrier surface recombination. It also appears that the higher MCL value (1987 µs) was found for an hydrogen flow rate of 9 sccm,

which slightly decreases with increasing the hydrogen flow rate (FH_2). We obtained a high quality nc-Si:H that can be used as a passivation layer of silicon substrates to improve its electrical properties. We prove this effect via the minority carrier lifetime that attains 1980 µs which is a high value, not reported before, indicating the crucial role of the deposited nc-Si:H thin film at the front surface. This behavior can be explained through the small reduction of Si–H bounds with FH_2 as previously mentioned, that reduces the performance of nc-Si:H thin films as a passivation layers.

4 Conclusion

In this paper, we prepared high quality hydrogenated nanocrystalline silicon thin films (nc-Si:H), deposited onto the front surface of silicon substrates using a MW-PECVD. We studied the influence of different hydrogen flow rates on morphological, structural, optical and optoelectronic properties of the prepared thin films and its effect on the effectiveness of its passivation role of the crystalline silicon substrates. The obtained result from XRD and Raman spectroscopy are strongly correlated showing that the films are nanocrystalline with preferential growth along the (111) plane for all deposited thin films. We found that increasing the hydrogen flow rate during the synthesis favors the dominance of the chemical annealing model which led to the extension of the crystallite size. A significant improvement of the minority carrier lifetime was obtained compared to untreated c-Si and to previous reports, indicating a significant reduction of the recombination activities in the treated crystalline silicon wafers. The passivation effectiveness was slightly affected by the effusion of the hydrogen with increasing the flow rate, and remains important improvement compared to other works.

Acknowledgements The authors acknowledge gratefully the help of Miss. Valerie Coudert for AFM surface analysis and Mr. Radhouene Allegui for spectroscopic Ellipsometry.

References

1. M. Konagai, in *15th Program Review Meeting of the National Center for Photovoltaics*, Denver, CO, 09–11 Sept 1998 p. 73
2. E. Leobandung, L. Guo, Y. Wang, S.Y. Chou, Appl. Phys. Lett. **67**, 938 (1995)
3. S. Tiwari, F. Rana, H. Hanafi, A. Hartstein, E.F. Crabbe, K. Chan, Appl. Phys. Lett. **68**, 1377 (1996)
4. J.-H. Shim, S. Im, Y. J. Kim, N.-H. Cho, Thin Solid Films **503**, 55 (2006)
5. J.P. Kleider, C. Longeaud, R. Bruggemann, F. Houze, Thin Solid Films **383**, 57 (2001)
6. S. Kumar, P.N. Dixit, C.M.S. Rauthan, A. Parashar, J. Gope, J. Phys. Condens. Matter. **20**, 335215 (2008)
7. S.B. Amor, H. Meddeb, R. Daik, A.B. Othman, S.B. Slama, W. Dimassi, H. Ezzaouia, Appl. Surf. Sci. **360**, 572–578 (2016)
8. S.B. Amor, R. Bousbih, R. Ouertani, W. Dimassi, H. Ezzaouia, Sol. Energy **103**, 12–18 (2014)
9. U. Graf, J. Meier, U. Kroll, J. Bailat, C. Droz, E. Vallat-Sauvain, A. Shah, Thin Solid Films **427**, 37–40 (2003)
10. R.E.I. Schropp, Thin Solid Films **403**, 17–25 (2002)
11. H. Jia, J.K. Saha, N. Ohse, H. Shirai, J. Phys. D **39**, 3844 (2006)
12. Y. Qin, T. Feng, Z. Li, Z. Sun, Appl. Surf. Sci. **257**, 7993 (2011)
13. R. Bousbih, W. Dimassi, I. Haddadi, S.B. Slema, P. Rava, H. Ezzaouia, Sol. Energy. **86–5**, 1300 (2012)
14. P. Zaumseil. Appl. Crystallogr. **48**, 528–532 (2015)
15. X.X. Wang, J.G. Zhang, L. Ding, B.W. Cheng, W.K. Ge, J.Z. Yu, Phys. Rev. B **72**, 195313 (2005)
16. X.X. Wang, J.G. Zhang, L. Ding, W.K. Ge, Phys. Rev. B **72**, 195313 (2005)
17. S.B. Amor, M. Atyaoui, R. Bousbih, H. Ikbel, R. Ouertani, W. Dimassi, H. Ezzaouia, Sol. Energy **108**, 126–134 (2014)
18. G. Yue, J. Lorentzen, J.D. Lin, D. Han, Q. Wang, Appl. Phys. Lett. **75**, 492 (1999)
19. A. Gajovic, D. Gracin, K. Juraic, J. Sancho-Parramon, M. Ceh, Thin Solid Films **517**, 5453 (2009)
20. J.-H. Shim, S. Im, N.H. Cho, Appl. Surf. Sci. **234**, 268–273 (2004)
21. E.A. Davis, J. Non-Cryst. Solids **1**, 198–200 (1996)
22. M. Katiyar, J.R. Abelson, Mater. Sci. Eng. A **349**, 304–306, (2001)
23. A. Matsuda, J. Non-Crystall. solids **338**, 1–12 (2004)
24. G. Lucovsky, R.J. Nemanich, J.C. Knights, Phys. Rev. B **19**, 2064 (1979)
25. L. Guo, J. Ding, J. Yang, G. Cheng, Z. Linga, N. Yuan, Appl. Surf. Sci. **257**, 9840 (2011)
26. J.H. Gu, Y.L. Ding, S.E. Yang, X.Y. Gao, Y.S. Chen, J.X. Lu, Acta Physica Sinica **58**, 4123–4127 (2009)
27. S.B. Li, Z.M. Wu, K. Yuan, N.M. Liao, W. Li, Y.D. Jiang, Acta Phys. Sinica **57**, 3126–3131 (2008)
28. B. Yan, G. Yue, J. Guozhen, J. Jeffrey, S. Guha, Sol. Energy Mater. Sol. Cells 111, 90–96 (2013)
29. R. Goswami, S. Ray, Appl. Surf. Sci. **282**, 615–623 (2013)
30. R.A. Sinton, A. Cuevas, Appl. Lett. **69**(17), 2510–2512 (1996)
31. A. Cuevas, D. Macdonald, Sol. Energy **76**, 255–262 (2004)
32. S. Ben Amor, R. Bousbih, R. Ouertani, W. Dimassi, Sol. Energy **103**, 12–18 (2014)
33. S. Ben Amor, M. Atyaoui, R. Bousbih, H. Ikbel, W. Dimassi, Sol. Energy **108**, 126–134 (2014)
34. S. Ben Amor, H. Meddeb, R. Daik, A. Ben Othman, B. Slama, S. Dimassi, W. Ezzaouia, Appl. Surf. Sci. **360**, 572–578 (2016)